ELSEVIER

Journal of Nuclear Materials 252 (1998) 200–208

journal of nuclear materials

Ion nitriding of titanium alpha plus beta alloy for fusion reactor applications

E. Rolinski [a,b,*], G. Sharp [a,b], D.F. Cowgill [c], D.J. Peterman [d]

[a] Advanced Heat Treat Corp., 1625 Rose Street, Monroe, MI 48162, USA
[b] Advanced Heat Treat Corp., Waterloo, IA, USA
[c] Sandia National Laboratories, Livermore, CA, USA
[d] McDonnell Douglas Corporation, St. Louis, MO, USA

Received 1 July 1997; accepted 9 October 1997

Abstract

The titanium alpha plus beta alloy, Ti–6Al–4V, has been plasma nitrided at 1033 K in pure nitrogen to produce a 9 μm thick surface nitride zone, followed by a 5 μm thick Al-enriched zone and a 100 μm thick nitrogen diffusion zone. X-ray diffraction and Auger electron spectroscopy indicate that the nitride zone consists of two layers: a thin TiN layer at the surface followed by a Ti_2N layer. In preliminary tests, the deuterium retention of nitrided titanium specimens was determined after exposure to fluences of 4×10^{25} m^{-2}, 60 eV D^+ ions at 440 K and of 2×10^{25} m^{-2}, 800 eV D^+ ions at 623 K. The results are compared to the retention found for similar exposure of the untreated alloy and to model simulations. Implications for the use of these materials in a fusion environment are discussed. © 1998 Elsevier Science B.V.

1. Introduction

Titanium-based alloys are attractive candidate materials for the construction of fusion reactors because of their low activation characteristics. However, since such alloys are embrittled by hydrogen under certain conditions, it is important to insure that Ti-based components meet the design criteria for strength, surface hardness, etc., during their service life. There have been several surface coatings/layers considered to protect titanium from fusion plasmas [1]. The idea of using a nitriding process for producing a protective barrier on titanium was described by Braganza et al. [2]. Titanium and titanium alloys form TiN and Ti_2N nitrides and an extended, nitrogen-enriched zone during nitriding. The nitride zones may reduce hydrogen uptake and at the same time provide the good abrasion resistance needed for certain applications as described by Braganza et al. [2] and Rolinski [3]. It has been speculated that the more dense Ti_2N nitride phase will be the most effective in inhibiting hydrogen from diffusing into titanium [2].

Plasma ion nitriding of titanium alloys has several advantages over gas and liquid nitriding methods, mainly relating to the facility of depassivation as described by Rolinski [3], Bell et al. [4], Zhow and Herman [5] and Metin and Inal [6]. Care must be taken that the nitriding temperature of alpha + beta titanium alloys does not exceed the beta transformation temperature in order to maintain low surface roughness as well as to achieve the proper TiN/Ti_2N thickness ratio (with the largest possible fraction of Ti_2N as discussed by Rolinski [3]). This paper reports a study of the surface structure of ion-nitrided Ti–6Al–4V and on the retention of deuterium in specimens exposed to deuterium plasmas.

2. Experimental details

2.1. Material and processing

The nitrided samples used in this experiment were fabricated from MIL-T-9047 titanium alloy. They were

---

[*] Corresponding author. Fax: +1-313 243 4066.

0022-3115/98/$19.00 © 1998 Elsevier Science B.V. All rights reserved.
PII S0022-3115(97)00325-5

machined into 6.4 mm thick, 25.4 mm radius disks. Ion nitriding exposures were performed in NDK (Nippon Denshi Kogyo Co., Japan) equipment in an atmosphere of 99.998% pure nitrogen. This equipment is normally used for the ion nitriding of steel production parts. The nitriding technique and parameters used in the process are described in more detail elsewhere [7]. Samples were degreased and rinsed with alcohol prior to nitriding. They were placed on a titanium cathode to avoid contamination of the surface by non-titanium atoms sputtered from the cathode, elements of the fixture, etc. The nitriding temperature was 1033 K. Nitriding was done for 148 h to produce thick nitride and nitrogen rich layers.

2.2. Ion exposure

The low-energy ion exposure was carried out in Sandia's deuterium plasma experiment (DPE), a magnetically-confined, rf-heated, plasma device capable of delivering a deuterium particle flux of about 10^{21} D^+ m^{-2} s^{-1} over 2800 mm^2, for extended periods. The DPE plasma is composed primarily of D_2^+ ions and has a positive potential of approximately 15 eV. During exposure, the sample was clamped to a copper plate by a stainless steel mask and biased at -105 V to give the ions a net energy of 120 eV. This resulted in an effective exposure to 60 eV D^+ ions. TRIM calculations [8] show that these ions have a penetration range of about 2 nm in TiN, TiO_2 or Ti. This range is less than the normal oxide thickness of 5–10 nm found on Ti. The sample was exposed to a fluence of $(3.6 \pm 0.4) \times 10^{25}$ D^+ m^{-2} using an average flux of 6.1×10^{20} D^+ m^{-2} s^{-1}. It was heated by the plasma to a constant temperature of about 440 K after 30 min of exposure. In addition to the deuterium plasma, the specimen was exposed to a background deuterium pressure of 0.5 Pa. Titanium reacts exothermically with hydrogen to form TiH_2 with an H_2 vapor pressure of about 10^{-4} Pa at 440 K. Thus, if the nitride and/or native oxide layers are not effective in protecting the titanium, this background pressure could produce a deuterium uptake even beyond 100% plasma-derived deuterium retention.

The higher-energy ion exposure was performed using dc glow discharges in Sandia's armor conditioning experiment (ACX) apparatus. Here the specimen was clamped to a copper plate and its edges were masked by a stainless steel holder. Prior to the plasma exposure, the specimen was vacuum baked in situ overnight at the exposure temperature, 623 K, to remove adsorbed water. The plasma exposed to an 800 eV fluence of 2.3×10^{25} $D^+ m^{-2}$ using an ion flux of about 1.2×10^{20} D^+ m^{-2} s^{-1}. The background deuterium pressure during this exposure was about 185 Pa. Here again the effect of the background pressure is of concern, especially since the ion energies are somewhat higher and can potentially sputter erode the protective nitride or oxide layers.

2.3. Characterization

As-nitrided specimens were examined by the use of optical and scanning electron microscopy, X-ray diffraction and Auger electron spectroscopy (AES). The AES data were obtained using a Physical Electronics PHI 600 with an electron beam energy of 10 keV and a beam current of 300 nA. Deuterium retentions were determined by thermal outgassing measurements. After plasma exposure, the nitrided specimens were cut in half along a diameter prior to outgassing to provide material for additional analysis. (Rapid oxidation of the cut by the ambient atmosphere and slow H diffusion at room temperature prevent any significant hydrogen isotope release resulting from this process.) Each specimen was outgassed in a passivated stainless steel tube furnace attached to the ACX apparatus. During sample transfer, the furnace was kept warm and purged with dry nitrogen gas to minimize contamination by air exposure. After rapid evacuation, the furnace temperature was ramped to 1123 K at 0.3 K/s, followed by a 'slow rise' to 1273 K, where it was held for several hours until the hydrogen partial pressures dropped to near background. During outgassing, hydrogen, deuterium and water vapor species were monitored with a UTI mass spectrometer. The mass spectrometer was calibrated by use of standard leaks and measured hydrogen flow rates from known volumes. Hydrogen and deuterium quantities were calculated from amplitudes of the mass peaks at 2, 3 and 4 amu and corrected for molecular fractionation in the ionizer. Water release was determined from the 18 amu peak. Residual H and D quantities within the samples were estimated by fitting exponentials to the decaying mass peaks. These residuals, which were less than 3% of the outgassed amounts, were added to get total quantities.

3. Results

3.1. As-nitrided structure

After nitriding, the color of the samples was gold, a characteristic of the TiN phase. An optical micrograph of a cross-sectioned specimen is presented in Fig. 1. The light etched zone indicates the penetration depth of nitrogen, approximately 100 μm. This thickness is comparable to the diffusion distance for N in α-Ti, $(2Dt)^{1/2} \approx 20$ μm, calculated using the diffusion coefficient D from Wasilewski and Kehl [9]. X-ray diffraction analysis of this zone showed the presence of both titanium nitrides, TiN and Ti_2N. Fig. 2 compares an X-ray spectrum of Ti–6Al–4V with that of the nitrided surface. As is evident, the major spectral peaks of the surface do not correspond with those of the alloy. Fig. 3 compares the X-ray intensities of standard JCPDS data for TiN and Ti_2N with the spectra obtained from the nitrided surface. Both nitrides contribute to the X-ray spectrum.

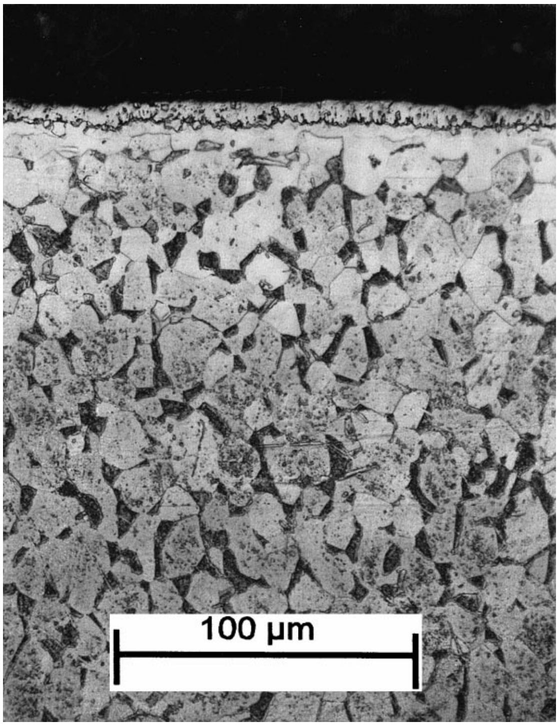

Fig. 1. Optical micrograph of the cross-section of plasma-nitrided Ti–6Al–4V etched with Kroll's reagent. The large grains appearing in the upper 1/3 are indicative of the nitrogen diffusion zone.

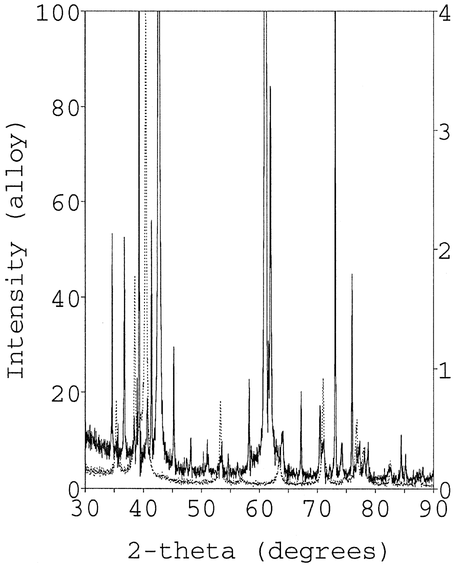

Fig. 2. Comparison of X-ray diffraction spectra obtained from a Ti–6Al–4V alloy (dotted line, left axis) with that obtained from the plasma-nitrided alloy surface (solid line, right axis). As is evident, the major spectral peaks of the nitrided surface do not correspond with those of the alloy.

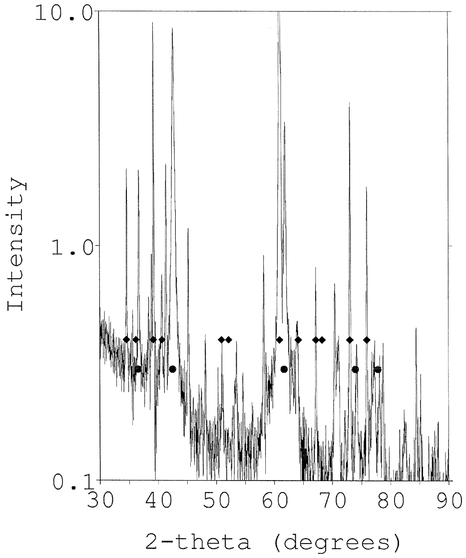

Fig. 3. X-ray spectrum of nitrided specimen compared to peak positions of TiN (JCPDS card #38-1420, shown with circles) and Ti_2N (JCPDS card #17-386, shown with diamonds). Comparison of peak positions shows that both of these nitrides contribute to the X-ray spectrum of the nitrided alloy. (Intensities of the standard spectra are not compared in the figure because one would not expect spectra from powdered or single-crystal standards to be the same as those from thin films, since the latter may bave preferred orientation, etc.) The data have been scaled such that the peak at about 62° has an intensity of 100.

Auger electron spectroscopy (AES) was used to further elucidate the near-surface composition. One complication for the AES analysis, however, is that the nitrogen-derived Auger electrons have the same kinetic energy as do some of the titanium-derived Auger electrons. This is illustrated in Fig. 4 where an electron energy spectrum obtained from the surface (after seven minutes of sputter etching) is compared with spectra obtained from points on a cross-sectioned specimen about 4 and 17 μm below the surface. The spectrum 17 μm below the surface appears similar to bulk Ti–6Al–4V. Clearly, the peak-to-peak amplitude of the nitrogen signal at about 380 eV in Fig. 4, which would normally be used for quantitative analysis, cannot be readily separated from the Ti signal. Fig. 5 shows an AES depth profile through the nitrided surface, where Al, as well as 'N and Ti' and Ti peak-to-peak signals (see Fig. 4) were measured. (The Al-derived signal from the KLL-Auger transition between 1381 and 1400 eV was used for the profile.) The profile suggests that there is a layered structure to the nitride zone, with a thin, nitrogen-rich layer on top. Depth profiling left an 11 μm deep crater, as determined by a stylus profilometer. During this profiling, it was noted that the change in composition, occurring after about 60 min of sputtering (see Fig. 5), was accompanied by a change in color from gold to silver. Considering

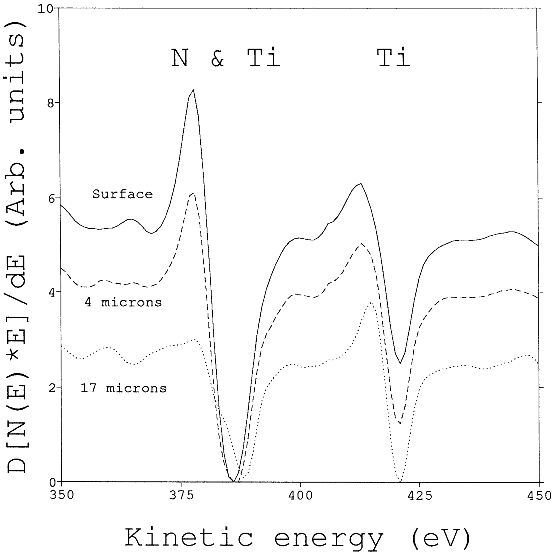

Fig. 4. Auger electron spectroscopy (AES) survey spectra obtained from the nitrided surface and from points 4 and 17 μm beneath the surface. The spectrum obtained from 17 μm is bulk-Ti-like and the comparison shows an increasing amount of nitrogen toward the surface and the fact that the nitrogen and titanium signals overlap, complicating quantitative analysis.

these results along with the X-ray results and assuming the same sputter rate for all materials, we conclude that there is a TiN layer ≤ 0.7 μm thick on top of a Ti_2N layer which is about 8 μm thick. This structure is nearly identical to that predicted by Braganza et al. [2].

The AES system was also used to examine cross-sections of the nitrided specimens. Fig. 6 shows a backscattered electron (BSE) image of such a cross-section. Two different layers are evident: one that is 8 μm thick (corresponding to the nitride zone discussed above) and another layer about 5 μm thick. Fig. 6 also shows an AES map of Al which indicates that this 5 μm layer is enriched in aluminum relative to both the nitride and the underlying bulk of the specimen. Fig. 7 shows an AES line scan obtained along the line shown in the BSE image of Fig. 6. The distance scale in Fig. 7 corresponds to the distance given in Fig. 6. The line scan consists of three lines, one due to Al, one due to Ti and one due to both N and Ti, where the plotted intensity is given by the difference in signal strength between the peak and background signals of the selected spectral regions. The peak and background energies, respectively, used in plotting the data were for Al: 1397, 1409 eV; for Ti: 418, 424 eV and for Ti and Ni: 381, 389 eV. (As mentioned above, there is no N signal that does not overlap with a Ti signal.) The 5 μm Al-enriched zone is again evident. In these cross-sectioned specimens, the AES signals give no clear evidence of a TiN layer. Higher resolution (lower beam current) modes of SEM, AES and BSE operation all failed to locate this layer along any portion of the cross-section. It is speculated that the TiN layer came off during specimen preparation. This specimen had been polished after coating with gold, electroplating with nickel (for edge retention) and mounting in a phenolic sample mount. Before being loaded into the ultra-high vacuum AES system, the specimen had been broken out of the sample mount. During this rather violent process, the gold and nickel layers separated from the specimen and it is therefore reasonable to assume that the TiN layer was also lost. It may be remarked that while this loss is consistent with a suspected large compressive stress within the TiN layer and somewhat weaker strength at the interface between the TiN and Ti_2N layers, it may also have implications regarding its durability for use in a fusion environment.

3.2. Deuterium uptake

Microscopic examination of the surfaces revealed no effects of the plasma exposures other than slight discoloration of the specimen exposed to 800 eV ions. After outgassing, however, the gold-looking color of both nitrided specimens was noticably reduced. The quantities of hydrogen and deuterium found in the samples are summarized in Table 1. Also shown are quantities obtained from a similar experiment performed with bare, un-nitrided

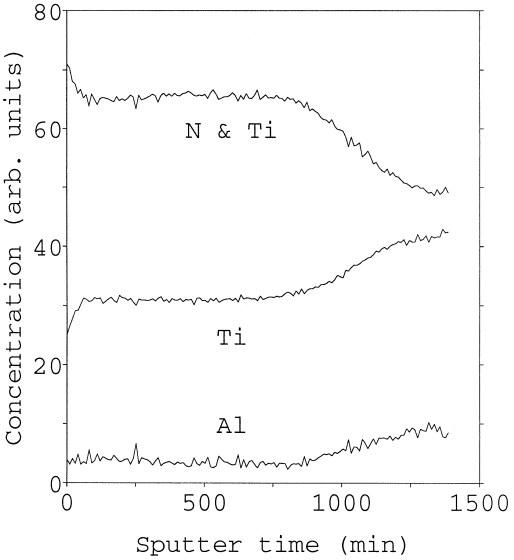

Fig. 5. AES depth profile through the nitrided surface. The concomitant increase in the aluminum signal (above the noise level), increase in the titanium signal and decrease in the 'N and Ti' signal marks the end of the nitride zone. Assuming a constant sputter rate through the various layers, the measured 11 μm deep sputter crater created during this profile, the X-ray results and these AES results suggest that there is a ≤ 0.7 μm thick TiN surface layer followed by an 8 μm thick Ti_2N layer. (The 'N and Ti' signal is due to N and/or Ti since they overlap.)

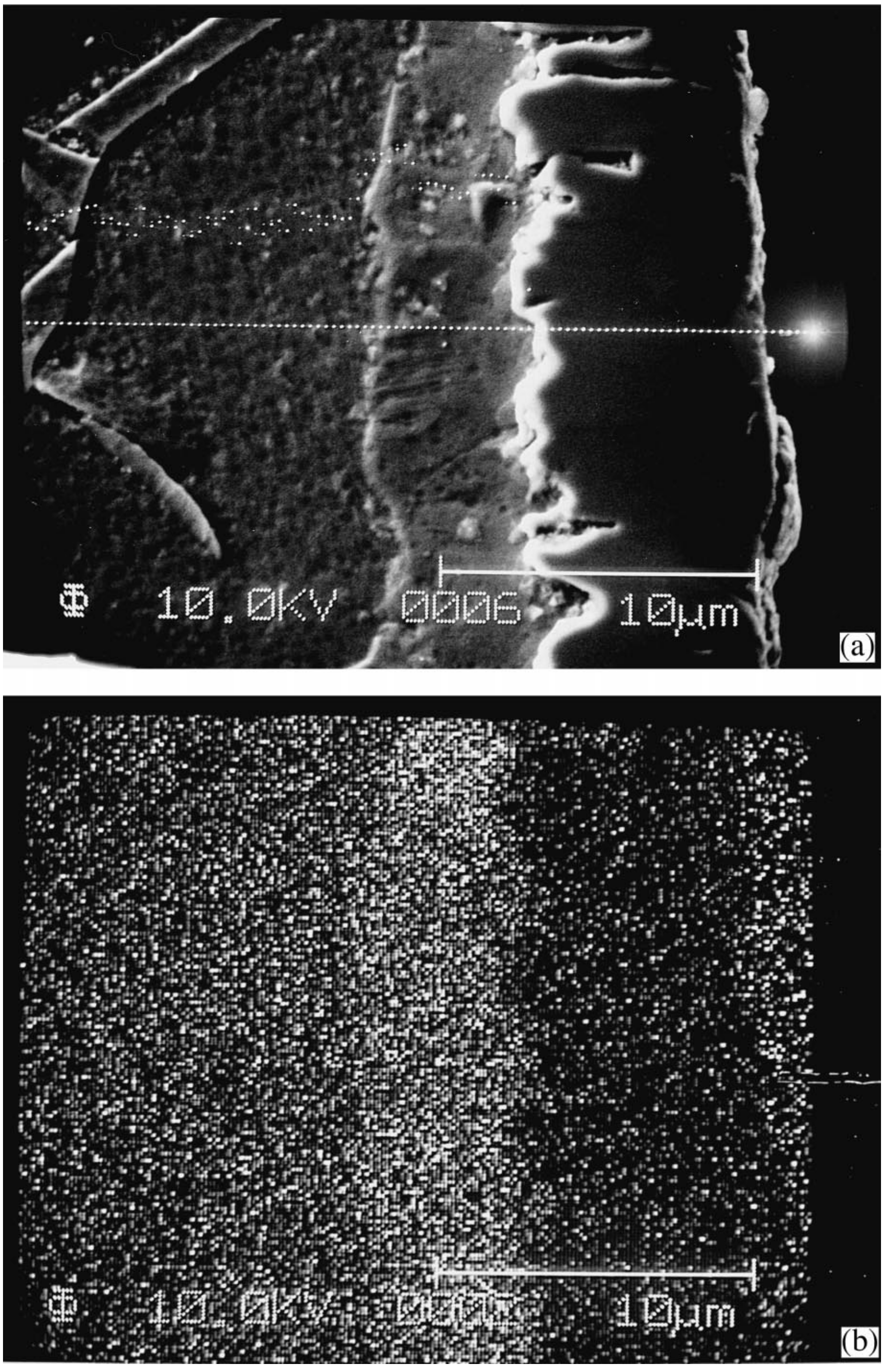

Fig. 6. Backscattered electron (BSE) image of the cross-section of the plasma-nitrided Ti–6Al–4V alloy (top) and a corresponding AES map of the aluminum distribution (bottom). The images indicate that there is an aluminum-enriched zone below the nitride zone. The dashed line in the BSE image marks the location of the line scan shown in the Fig. 7.

Ti–6Al–4V, but from a different, thinner lot of material. The quantities are stated as atom fractions, in appm, relative to Ti atoms. They are calculated from the sample masses after outgassing using the Ti–6Al–4V composition. The ion exposures, given as D/Ti, used for each specimen were many times the quantities found. Thus the samples retained only a small fraction of the incident ions. Measured amounts of hydrogen (1590 appm ≈ 34 wppm)

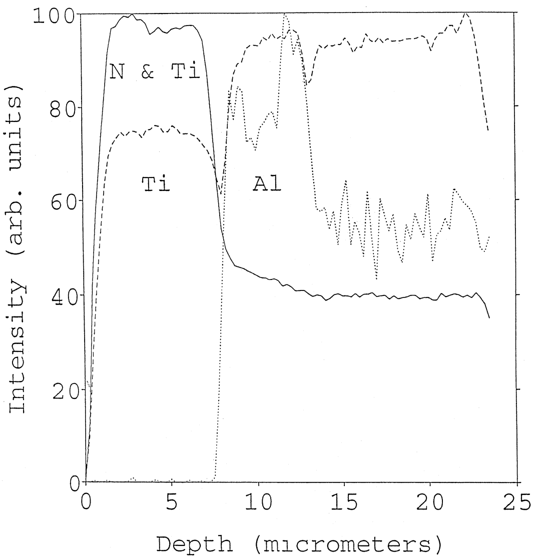

Fig. 7. AES line scans across the cross-section shown in Fig. 6. The distance scale on the *x*-axis corresponds to the distance shown in Fig. 6. The line scans indicate an 8 μm width for the nitride zone and a 5 μm width for the Al-enriched zone.

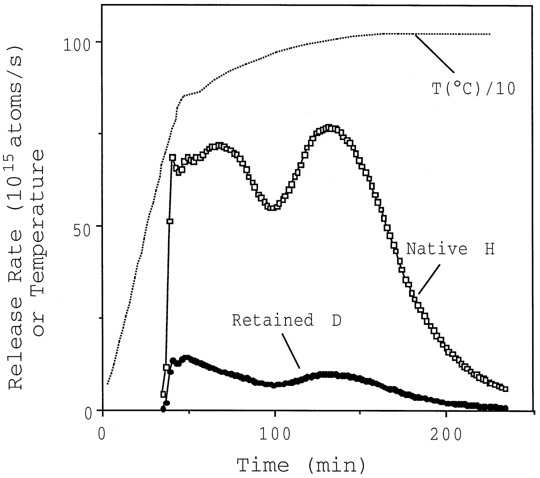

Fig. 8. Hydrogen and deuterium desorption spectra from nitrided Ti–6Al–4V exposed to the 60 eV deuterium plasma at 440 K. Release of roughly half of each isotope appears delayed in time.

are consistent with those quantities normally found in unexposed Ti alloys [9,12]. The larger H concentration found in the bare sample may be due to the different material lot or the fact that it did not experience the high temperature nitriding treatment.

Hydrogen and deuterium outgassing spectra for the nitrided specimen exposed to 60 eV ions are presented in Fig. 8. Release of both isotopes began around 650°C. The absence of D release below this temperature suggests that little implanted D resides weakly-bound within the nitride layer. Small, transient gas bursts were observed at 650–670°C, indicative of cracking or dissolution of the surface layers. The release rates rise rapidly at this temperature and produce a broad peak centered at about 800°C. Release rates for both isotopes increase again around 900°C and produce a second broad peak with an inventory which includes roughly half of each species. The release of H_2O, HDO and D_2O was also monitored and it was determined that the total amount of H and D contributed by dissociation of water was negligible.

Deuterium outgassing spectra for all three samples are plotted in Fig. 9. The onset of release appears shifted to slightly higher temperature for the nitrided specimens. This shift may be due to a higher temperature requirement for dissolution or cracking of the nitride layer than of the oxide layer. (The shift may indicate a slightly greater ductility or durability of the nitride layer than the oxide.) There is also significant difference in the widths of the spectral peaks. Some of this difference may result from a small change in temperature ramps; however, most is believed to be due to the different sample thicknesses. At 700–900°C the diffusion coefficient for deuterium in α-Ti is about 5×10^{-5} cm^2/s [9]. Thus the time to diffuse 0.5 mm, half the thinner sample thickness (release from both sides), is $l^2/2D \approx 30$ s. Increasing the sample half-thickness to 3 mm increases this diffusion time to about 20 min. The peak widths in Fig. 9 clearly reflect these diffusion times. (Unfortunately, a bare 6.4 mm sample was not available for comparison.) It is argued below that the

Table 1

Outgassing results for three deuterium-plasma-exposed Ti–6Al–4V specimens, two of which had been ion-nitrided. Exposures: 60 eV at 6.1×10^{20} D^+/m^2 s, 440 K for 17 h and 800 eV at 1.5×10^{20} D^+/m^2 s, 623 K for 24 and 48 h

(appm)	Nitrided, 6.35 mm 60 eV, 440 K, 17 h	Nitrided, 6.35 mm 800 eV, 623 K, 48 h	Bare, 1.0 mm 800 eV, 623 K, 24 h
Exposure D/Ti	80 000	50 000	163 000
H/Ti	1590	2671	4446
D/Ti	220	1003	1492
Simulation, no coating	44 000 (not saturated)	7940 (saturated)	7940 (saturated)
Observed D simulation	0.005	0.19	0.43

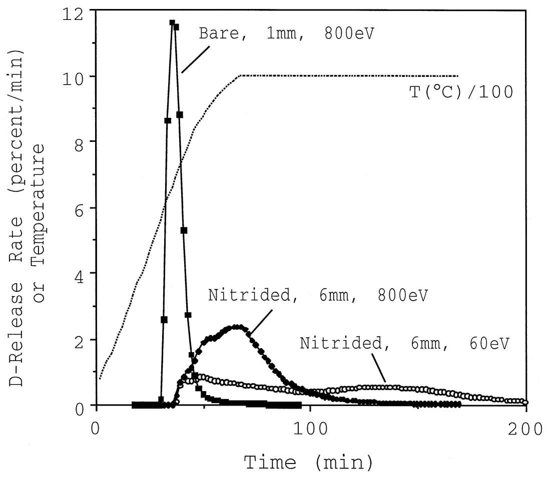

Fig. 9. Deuterium desorption spectra from plasma nitrided Ti–6Al–4V after exposure to 60 eV D^+ ions (from Fig. 8) and 800 eV D^+ ions, compared to the spectrum from untreated Ti–6Al–4V exposed to 800 eV D^+ ions. (The temperature ramp here is for the 800 eV-exposed specimens and differs slightly from that shown in Fig. 8.) Deuterium is released earlier for the untreated specimen.

differences in the desorption spectra may be due to thinner nitride layers present on the more aggressively sputtered specimen.

4. Discussion

Retention of the gold color by the specimen exposed to 60 eV ions is not surprising since this ion energy is too low to produce significant sputter erosion. The Ti sputtering coefficient for 60 eV D^+ ions is estimated to be 0.0005 Ti/ion at normal incidence [10]. For the test fluence, sputtering should produce an erosion of about 2×10^{22} Ti/m^2 or about 350 nm. This is an order of magnitude less than the thickness of the thin TiN layer and is also less than the sample roughness. For 800 eV ions, however, the sputtering is much greater. The Ti sputtering coefficient for 800 eV D^+ ions is 0.018 Ti/ion [10]. For the test fluence, this gives an erosion of about 7 μm. (The erosion might be slightly less for TiN, compared to Ti, based on binding energy considerations [11].) Thus sputtering should have removed all the TiN and some of the Ti_2N layer from the specimen exposed to 800 eV ions, but removed neither layer from the specimen exposed to 60 eV ions.

Although outgassing was done primarily to determine the net quantities of deuterium introduced into the samples by the ion exposures, some additional information can be gleaned from the thermodesorption spectra. As mentioned above, the onset of desorption of hydrogen from the samples is believed to reflect the characteristics for dissolution of the coating rather than the release of hydrogen from trap sites within the nitride layers. Several features of the second peak in Fig. 8 suggest it resulted from a time delay associated with a surface permeation barrier. First, it is difficult to envision a 1200 K ‘deep’ trap in these materials which becomes populated during exposure at 440 K but not at 623 K. Second, the release of H and D with the same peak characteristics indicates local mixing of the isotopes. This requires atomic mobility prior to release. Local mixing of hydrogen trapped at interstitial N in the N-rich α-Ti or in the nitride layers should occur when the nitrogen becomes mobile, which is somewhat below the nitriding temperature, 1033 K. Braganza et al. [2] have proposed that hydrogen isotope transport is significantly reduced through the crystalline Ti_2N layer. They also argue that the growth of interstitial sites within Ti_2N will remove its effectiveness in blocking H and D transport. Thus the second peak may be associated with the time required for this growth. Fig. 9 shows that a second peak is indeed absent from the sample sputter eroded sample by the 800 eV flux. This second peak may also be associated with a change in the hydrogen recombination rate at the surface. Changes in the surface N-concentration can rapidly alter the recombination rate. A significant increase will likely occur as fresh Ti metal becomes exposed on the surface. Increased interdiffusion time is required to produce a substantial change when the thick nitride layers are present. Finally, it should be noted that the existence of this second peak may be a consequence of the slightly different temperature ramp used for this sample.

The maximum amount of $H + D$ found in the specimens was 5940 appm, assuming uniform distribution. This corresponds to 130 wppm H and is still almost an order of magnitude less than that which is reportedly [9,12] required to affect the mechanical properties of Ti–6Al–4V. It should be noted that the fluence for fusion reactor applications can be significantly higher than that employed in these experiments. In a tokamak environment there are two sources of deuterium ions, the operating plasma and the glow discharge conditioning plasma. The former source generates a higher ion fluence, but many titanium components are better shielded from this plasma. For the proposed tokamak physics experiment (TPX), for example, the D^+ fluence was estimated to be between 10^{25} and 10^{27} m^{-2} at energies between 100 and 300 eV[13]. Tokamak plasmas also produce large fluxes of neutral D atoms, which are not confined by the magnetic fields.

It is particularly interesting that the bare, but oxidized, Ti–6Al–4V specimen did not pick up a large amount of deuterium. Calculations [14] have indicated that deuterium pressures more than 1000 times *less* than the background pressure used during the 800 eV exposure should produce a deuterium concentration of about 20 000 appm if no protective oxide layer is present. Apparently, even in this sputtering environment, re-oxidization must have been sufficiently rapid to maintain the protective surface oxide.

This is not too surprising, since re-oxidation requires an oxide impurity partial pressure of only about 10^{-5} Pa, or less than 1 ppm in deuterium.

The deuterium uptake and retention for unprotected Ti–6Al–4V was simulated for each set of exposure conditions using the DIFFUSE code [15]. In these simulations, no release was allowed at the back surface and no external gas pressure was used at the front surface, in accordance with the observations above. The results of the simulations are shown in Fig. 10 and included in Table 1. The simulation shows D retention is still increasing for the exposure at 440 K, but is saturated for the exposures at 625 K. Table 1 also gives the ratios of the observed D concentration for each specimen to the simulated concentration without plasma protection. A smaller ratio indicates better plasma protection. Here, for the simulations which are in saturation, the simulated concentrations (denominators) were reduced by the native H, since this H presumably reduces the available volume (solubility) for deuterium. A comparison of the two samples exposed at 623 K shows that under the saturation condition, the nitride layer provides 2–3 times better protection from D uptake than the native oxide. This is true even under the test conditions where a substantial amount of the nitride layer is sputtered away. The simulation also shows that while saturation takes longer to achieve at 440 K, a higher saturation level can be expected. This is due to the higher solubility of H in Ti at the lower temperature.

It appears that there was no significant decrease in the amount of native hydrogen found in the bare specimen after exposure to the 800 eV ions. With the large saturation effect limiting the deuterium retention, one might expect some deuterium–hydrogen exchange to occur, reducing the H concentration. One can argue that perhaps the difference between the hydrogen concentrations in the nitrided specimens is due to isotope exchange in the near surface region of the 440 K specimen only, where higher local D concentrations would occur. One could also speculate that the high temperature plasma nitriding process might be expected to decrease the hydrogen concentration. However, clearly an insufficient number of samples were measured to evaluate this apparent specimen-to-specimen variation in the measured H concentration.

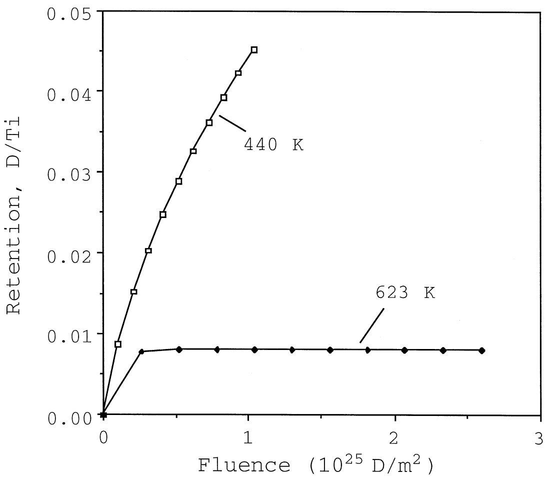

Fig. 10. Simulated uptake from deuterium plasma exposure of uncoated α-Ti at 440 and 623 K, computed using the DIFFUSE code with zero gas pressure at the surface.

Table 2
Comparison of glow discharge conditioning (GDC) parameters for the TPX design [13] with the parameters used in the 800 eV D^+ ion exposures of this experiment

	GDC	800 eV exposure
Ion flux	2×10^{18} m^{-2} s^{-1}	1×10^{20} m^{-2} s^{-1}
Ion fluence	2×10^{25} m^{-2}	2×10^{25} m^{-2}
Ion energy	400 eV	800 eV
Temperature	623 K	623 K
H(D) partial pressure	< 3 Pa	~ 185 Pa

The observation that a surface oxide layer was always present in this experiment is encouraging for those contemplating the use of titanium components in tokamak reactors. The parameters used here, particularly the ion flux, were more aggressive than those anticipated in such a reactor during glow discharge conditioning (GDC). For example, Table 2 compares GDC parameters for the TPX design [13] with the parameters used here. On the other hand, if GDC is done with heavier gases, even He, sputter erosion will be considerably higher and one could not be assured, without further experimentation, that the oxide protection would remain intact. Also, the partial pressure of oxygen in the vacuum vessel used in this experiment may be somewhat larger than would be achieved in a well-conditioned tokamak vessel, making oxide layer regeneration more rapid in the present experiment than in a tokamak. This is particularly likely for Be-lined machines which aggressively getter oxygen-bearing contaminants. It is also likely that the boronization procedures used in carbon-lined machines will produce TiB_2 surface layers and that such layers may be as effective at inhibiting plasma uptake as the nitride layers tested here. It must be cautioned, however, that the surface reactions which occur with typical boronization gases (e.g. B_2H_6) are likely to increase the hydrogen injection into underlying titanium during the boronization process. Additional experimental measurements are strongly recommended in this area.

5. Conclusions

Plasma ion nitriding of Ti–6Al–4V resulted in a layered structure consisting of a thin (≤ 0.7 μm) surface TiN layer, followed by an 8 μm Ti_2N layer, a 5 μm Al-enriched layer and a 100 μm N-enriched zone. These nitride layers are known to protect titanium from mechanical abrasion. The experiments reported here show that the nitride layers are just as effective at inhibiting gaseous hydrogen uptake as the normally-present oxide layer and perhaps more thermally durable. The experiments indicate that nitride layers also provide additional protection from low-energy deuterium plasmas. Deuterium uptake from plasma exposure at 440 K was found to be 200 times slower than predicted to occur on unprotected Ti–6Al–4V and uptake at 623 K was found to saturate at less than half the level found with normal-oxide protection only. These experiments and exposure simulations demonstrate the interplay of the various plasma–material interactions. They show the importance of evaluating behaviors under both (a) the specific test conditions required for the application and (b) for a range of parameters to provide an understanding and confidence in the results.

Acknowledgements

The authors are indebted to R.A. Causey, Sandia National Laboratories for assistance with the DIFFUSE code calculations. This work was supported under General Atomics Subcontract No. SC H418203.

References

[1] M. Davis, J. Nucl. Mater. 85&86 (1979) 1063.
[2] C. Braganza, H. Stussi, S. Veprek, J. Nucl. Mater. 87 (1979) 331.
[3] E. Rolinski, Mater. Sci. Eng. A 108 (1989) 37.
[4] T. Bell, H.W. Bergmann, J. Lanagan, P.H. Morton, A.M. Staines, Surf. Eng. 2 (1986) 133.
[5] K. Song Zhow, H. Herman, Wear 80 (1982) 101.
[6] E.S. Metin, O.T. Inal, Light Metal Age Dit. 26 (1989).
[7] E. Rolinski, Mater. Sci. Eng. 100 (1988) 193.
[8] J.P. Biersack, L.G. Haggmark, Nucl. Instrum. Meth. 174 (1980) 257.
[9] R.J. Wasilewski, G.L. Kehl, Metallurgia 50 (1954) 225.
[10] Y. Yamamura, H. Tawara, National Institute for Fusion Science Research Report, NIFS-DATA-23, 1995, p. 30.
[11] H. Conrad, Progress in Material Science, vol. 26, Pergamo, Oxford, 1981, p. 123.
[12] J.W. Davis, M.A. Ulrickson, R. A Causey, J. Nucl. Mater. 212–215 (1994) 813.
[13] D.J. Peterman, Tokamak Physics Experiment Plasma Facing Components, Close-Out Status Report, R&D Task 21: Hydrogen Barrier Coatings For Protection of Titanium-Alloy Shields in TPX, McDonnell Douglas Report # MDC 95P0070, 29 Sept. 1995 and references therein.
[14] R.A. Causey, D.F. Cowgill, Deuterium Uptake in Titanium Alloys, presented at Oak Ridge National Laboratory, March, 1995.
[15] M.I. Baskes, DIFFUSE 83, SAND83-8231, Sandia National Laboratories, 1983.